JOURNAL OF GEOPHYSICAL RESEARCH VOLUME 67, NO. 1 JANUARY 1962

New Experimental Evidence of the Effect of Magnetic Storms on the Magnetosphere

D. L. CARPENTER

Radioscience Laboratory, Stanford University, Stanford, California

Abstract. New methods of whistler analysis have recently been developed and have been used to study the effect of magnetic storms on the magnetosphere. It is found that whistler observations preceded within 72 hours by a 3-hour K_p level of 6 or more show relatively low values of time delay at typical whistler nose frequencies. During the main phase and recovery phase of several severe magnetic storms, depressions in nose frequency time delays on the order of 2:1 are observed.

Evidence is presented that the depressions in whistler delays may be interpreted as reductions in electron density in the magnetosphere. The depression in electron density during several severe storms is then on the order of 4:1.

An intensive study of whistler data has recently been made by the author, with particular attention devoted to data from magnetically disturbed periods. As a result of this study, there is available for the first time extensive experimental evidence on the effect of magnetic storms on the magnetosphere. This is a preliminary report on the principal features of the experimental evidence.

Background of the investigation. The pioneering work on whistlers by *Storey* [1953] showed that portions of the VLF energy from a lightning flash can propagate between the hemispheres along a dispersive path following approximately the lines of force of the earth's magnetic field. In this early work, Storey discussed the use of whistlers to obtain information on electron density in the outer ionosphere, or magnetosphere.

Later investigators have been very much interested in the problem of deriving information on electron densities from whistlers. The nose whistler phenomenon was investigated [*Helliwell, Crary, Pope, and Smith,* 1956], and the theory developed showed that f_n, the nose frequency of a whistler trace (frequency of minimum time delay), provides information on the location of the whistler path, e.g., latitude of path endpoint, while t_n, the time delay at the nose frequency, is proportional to the square root of the scale factor of the ionization distribution along the path [*Smith,* 1960]. Whistlers were recognized to be particularly advantageous for study of the magnetosphere because the tenuous ionization at the top of the path provides the principal contribution to the group delay.

The nose whistler work and related studies implied that if nose whistlers were recorded regularly on a world-wide basis, it would be possible to map the world-wide variations in the density levels of the magnetosphere. This was one of the ideas behind the ambitious IGY-IGC whistler program, although it was known that actual nose whistlers (see Fig. 1, top) would be observed relatively infrequently in comparison to ordinary whistlers, which follow the same dispersion law, but do not exhibit an observable nose on the spectrographic records.

During the IGY-IGC period, hundreds of thousands of whistlers were recorded. The author has examined spectrographic records (sonagrams) of several thousand of those received by the whistlers-west network, and has made detailed measurements on about six hundred examples. (The whistlers-west IGY-IGC network included the following stations: Anchorage, Boulder, College, Dunedin, Kotzebue, Macquarie Island, Seattle, Stanford, Unalaska, and Wellington, with associated stations at Byrd and Pole stations in Antarctica.)

Development of methods of analyzing whistler records. One of the principal problems faced in scaling a whistler is the identification on the spectrograms of the causative atmospheric. Fortunately, the bulk of the whistlers-west records exhibit relatively low background atmospheric

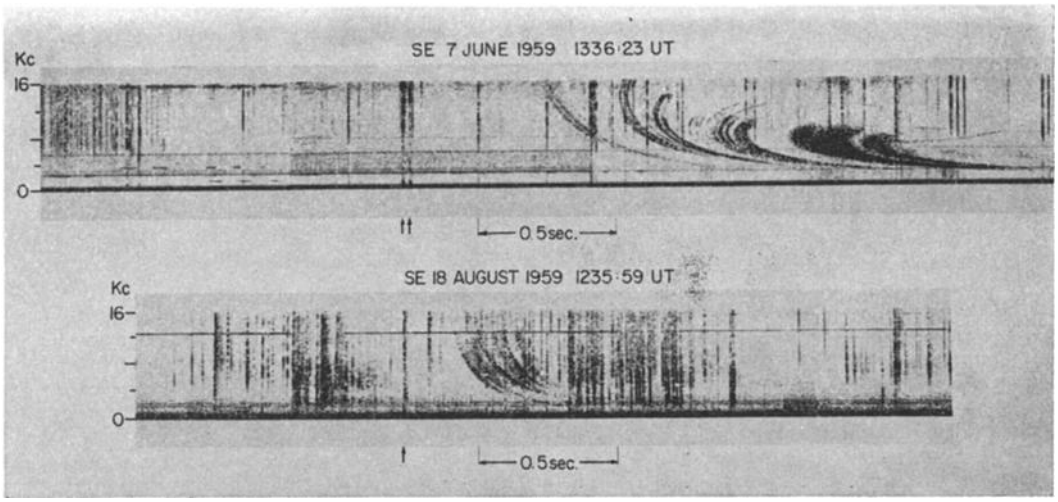

Fig. 1. Top: Two closely spaced multicomponent nose whistlers. Bottom: Multicomponent whistler observed following a severe magnetic storm.

rates. The author has found it possible to identify accurately the sources of several thousand short whistlers, the majority of which were recorded during local night. The methods used include: comparison of several whistlers recorded in a single run, comparison of the same event recorded at spaced stations, and other techniques not dependent upon particular theories of the frequency vs. time behavior, or dispersion law, of whistlers [*Carpenter*, 1960]. In addition to these 'independent' methods, analytical methods based on whistler trace shape have recently been developed [*Smith and Carpenter*, 1961]. The latter give approximate information on whistler sources, and are particularly useful in support of the independent techniques. The point to be stressed here is that short whistler sources can be identified in the majority of cases observed in the whistlers-west network during local night (and often during daytime). In other words, whistler-producing atmospherics propagate in the earth-ionosphere waveguide to the opposite hemisphere, and are readily identified on sonagrams. In Figure 1, the sources of the whistlers are indicated by arrows and are seen to be well defined. Even at Byrd station (70°S), short whistler sources may frequently be identified on the records.

The bulk of the whistler measurements carried out by the Stanford workers during the IGY-IGC period were limited to the recording of time delays at 5 kc/s. Smith scaled a number of nose whistlers during this period, and as a result of his work on nose whistler theory [*Smith*, 1960], it became possible to calculate the values of f_n and t_n for many well defined whistler traces that do not exhibit an observable nose on the records [*Smith and Carpenter*, 1961]. The experimental error in this new scaling method has been studied and found to be relatively small (see below), and the method has been checked for consistency with actual nose traces. The extension of nose whistler analysis to well defined ordinary whistler traces increased by at least an order of magnitude the quantity of data which can be applied to the study of electron density in the magnetosphere.

Initial results. In conversations with R. A. Helliwell and A. J. Dessler in the summer of 1960, it was suggested that the new methods of analysis be applied to whistlers recorded during the period of the severe magnetic storm of August 16–17, 1959. This was done, and it was found that time delays at typical whistler nose frequencies were substantially reduced during the main phase and the recovery phase of the storm, particularly on August 18. Other disturbed periods were investigated, and it was found that large reductions in time delay occurred in the late phases of several storms during which the K_p index reached 8 or 9, as well as for several lesser disturbances. A report on

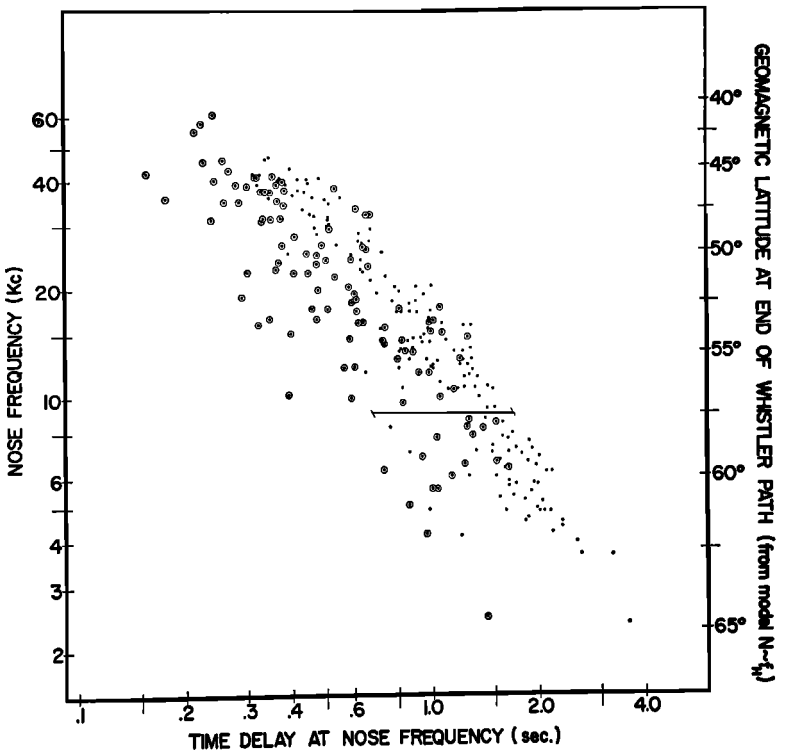

Fig. 2. Values of (f_n, t_n) illustrating the behavior of whistler data for the period October 1957 through April 1961.

these findings was made by the author at the joint URSI-IRE meeting in Washington, D. C., in May 1961.

Further investigation. After the initial work on storm periods, it became necessary to study the behavior of whistlers during other periods, so that the storm-period variations could be placed in perspective.

Accordingly, measurements of f_n and t_n were obtained for some 128 days during the period October 1957 through April 1961, with the bulk of the measurements from the period November 1957 through August 1959. The results are plotted in Figure 2 in coordinates of log f_n vs. log t_n, a type of presentation used by *Smith* [1960]. Figure 3 shows the data from Figure 2 covering the period from June 1, 1959, to September 8, 1959.

The graph of log f_n vs. log t_n. A few explanatory remarks on Figures 2 and 3 are in order. A typical multicomponent nose whistler shows a reasonably smooth decrease in f_n with t_n, as illustrated in the upper sonagram of Figure 1. A plot of f_n vs. t_n for such a whistler forms a reasonably smooth curve on a log-log graph. This is illustrated by several of the examples in Figure 3 (points connected by lines).

The physical significance of the plots is emphasized by the latitude scale included on the right. This is a scale of θ_0, the geomagnetic latitude of the path end-point of a whistler having nose frequency f_n. The f_n–θ_0 relation used in the figures was calculated by *Smith* [1960] for the gyrofrequency model of electron distribution in the outer ionosphere. In this model, N, the number density of electrons, is proportional to f_H, the electron gyrofrequency.

Although it is necessary to assume a density model in order to make certain calculations, it is possible to make a physical interpretation of the f_n vs. t_n graph without assuming a particular model of electron distribution in the magnetosphere. Most theoretical models lead to an f_n–θ_0 relation not greatly different from the one illustrated [*Smith*, 1960], so that, to a first approximation, the f_n–θ_0 relation may be con-

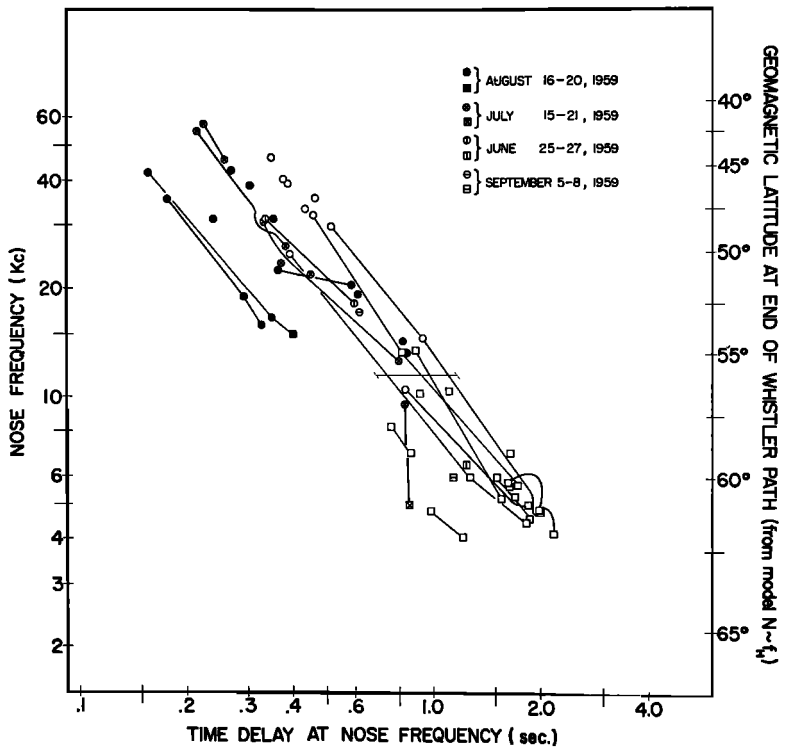

Fig. 3. Values of (f_n, t_n) illustrating the behavior of whistler data for the period of June 1, 1959, to September 8, 1959.

sidered model-independent. Since t_n is proportional to the square root of the scale factor of the ionization distribution along the whistler path, the variations of t_n may be studied without specifying the particular form of the electron distribution function. A 2:1 change in t_n at fixed f_n may be interpreted as a 4:1 change in density levels along the relevant whistler path, provided that the parameters of the magnetosphere do not change concurrently in such a way as to require drastic changes in the dispersion law of whistlers.

Description of data represented in Figure 2. Whistler activity over an extended period is illustrated in Figure 2. Each dot represents a single whistler trace, and there are a total of 262 dots for 128 recording days, an average of 2 per day. The number of values of (f_n, t_n) representing a single UT day was limited by selecting at most one whistler per day from each of two stations. If these were multicomponent whistlers (as in Fig. 1), at most three values from a single whistler were taken—the highest and lowest values of f_n, and the intermediate value falling nearest to midway between the other two on the log-log plot. Thus the maximum number of dots for a single day is 6.

When several whistlers were available from a station for a day, the whistler exhibiting the widest range of f_n values was selected. If two or more were similar in this respect, the results involving the smallest experimental error were used. The bulk of the points above 15 kc/s were obtained by extension methods, while nearly all those below that level are the result of direct observations of noses.

Table 1 lists the UT days represented in Figure 2. The various stations and their relevant lists of recording days are indicated opposite the appropriate months. Relatively large numbers of observations were made during certain periods because of particular objectives, such as obtaining pre- and post-storm material to make possible a proper evaluation of storm-time phenomena.

A circled point in Figure 2 indicates that a

3-hour K_p level of 6 or more was reached at some time during the 72 hours preceding the whistler. The observations marked in this way are listed in Table 2. The experimental errors listed in Table 2 will be discussed below.

Discussion of Figure 2. The data presented in Figure 2 tend to group in a broad band that slants downward to the right. The band appears to have a slight downward curvature. The higher values of t_n, representing higher electron density levels, show a fairly well defined right-hand or upper limit, particularly in the region $\theta_0 = 45°$ to $\theta_0 = 60°$. The values of (f_n, t_n) for $\theta_0 > 60°$ are relatively few in number and are not distributed sufficiently over the seasons of the year to be properly comparable with the other data.

The left side of the distribution of points, representing lower levels of ionization, does not exhibit a well defined limit, but instead shows a gradual decrease in the number of observations down to the lowest values of t_n observed.

On the basis of Figure 2, several observations may be made about the data. Over the latitude range of roughly 45° to 60°, the maximum and minimum values of t_n (for fixed f_n) exhibit a ratio of about 4:1. In this latitude range the upper limit of t_n is rather well defined. Values of t_n near this upper limit are observed primarily during the months October through April (compare with Fig. 3 for June-September data), a fact that is consistent with the annual variation shown by recent whistler measurements [*Smith*, 1960; *Helliwell and Carpenter*, 1961]. If the 90 per cent range of t_n for fixed f_n is estimated as an indication of the over-all variation of the

TABLE 1. Recording Dates of Whistler Data Illustrated in Figure 2

	UT days and Recording Station*				
Month	1957	1958	1959	1960	1961
Jan.		5, 11, 30, 31 (KO); 13, 14, 27 (ST); 13, 14 (WE)		21 (ST)	17, 18, 25, 29 (SE); 5. 24, 29 (ST)
Feb.		2, 10, 13, 24, 27 (BO); 5 (KO); 1, 5, 11 (SE); 5 (ST); 12 (WE)	9 (ST)		
Mar.			19 (UN)	30, 31 (ST)	4, 9, 10, 12, 24, 25, 30 (ST)
Apr.		15, 17, 23, 25 (SE)	9 (SE); 11, 27 (UN)	1 (BY); 3 (SE); 1, 2, 3, 4, 5, 10, 17, 25 (ST)	17 (SE)
May		20, 21, 31 (SE); 1, 2, 17 (ST)		2 (ST)	
June		20 (EL); 1, 12, 20, 25 (SE); 14 (ST)	6, 7, 9, 10, 22, 25, 27 (BY); 7 (SE); 4 (ST)	16, 29 (BY); 1, 3, 8, 12 (ST)	
July		4 (UN); 11 (SE)	18 (BO); 8, 19, 20, 23 (BY); 11, 14, 15, 17, 23, 31 (ST)	15 (SE)	
Aug.			18 (BO); 6, 8, 9, 15, 16, 17, 19 (BY); 18, 20 (SE); 19 (ST); 17, 19, 20 (WE)		
Sept.		4, 5, 7 (BO); 10 (UN); 3, 6, 7 (WE)	5, 8 (BY)	26 (ST)	
Oct.	4 (BO)	1, 11, 17, 19, 22, 23, 24, 25, 27, 30 (UN)		4, 6. 7. 8 (ST)	
Nov.	16, 17, 24, 28 (ST)	20 (SE); 1, 2, 3 6, 9, 11, 13, 20,23 (UN)	23 (SE)		
Dec.	1, 4 (ST)	11 (UN)			

* Station codes: Boulder (BO); Byrd (BY); Ellsworth (EL); Kotzebue (KO); Seattle (SE); Stanford (ST); Unalaska (UN); Wellington (WE).

TABLE 2. Whistler Observations Preceded within 72 Hours by a 3-hour K_p Level of 6 or Greater

Date	UT	Station	f_n, kc	f_n Error +	f_n Error −	t_n, sec.	t_n Error −	t_n Error +	Actual Nose
Nov. 28, 1957	1335:24	ST	23.0	2.1	1.8	.669	.029	.023	x
Dec. 1	1335:17	ST	32.0	5.8	4.2	.660	.052	.036	
Feb. 11, 1958	0835:86	SE	10.2	.7	.7	.397	.019	.012	
Feb. 12	0735:35	WE	26.0	3.1	2.3	.643	.036	.025	
Feb. 13	1035:unc	BO	15.6	.2	.2	.741	.016	.016	x
Apr. 17	1135:26	SE	10.5	.9	.8	1.160	.040	.038	
May 31	0135:07	SE	13.3	.3	.3	.883	.050	.050	x
	0135:07	SE	11.7	.3	.3	.984	.050	.050	x
	0135:07	SE	10.0	.3	.3	1.063	.050	.050	x
June 1	0635:36	SE	14.3	.4	.4	.733	.016	.016	x
June 12	1035:19	SE	14.0	.3	.3	.742	.016	.016	x
July 11	0635:50	SE	7.7	.7	.7	1.033	.100	.100	x
Sept. 4	1235:18	BO	26.5	11.3	5.7	.495	.085	.058	
Sept. 5	1135:58	BO	24.8	2.3	1.7	.478	.023	.015	
Sept. 6	1335:24	WE	60.7	42.3	17.0	.243	.070	.047	
	1335:24	WE	37.5	4.1	3.2	.388	.025	.015	
	1335:24	WE	29.5	5.6	3.9	.518	.045	.030	
Sept. 7	1135:33	BO	41.2	2.9	2.9	.360	.018	.010	
	1135:33	BO	39.0	8.5	5.5	.369	.040	.026	
Sept. 7	1435:86	WE	40.8	10.2	6.5	.325	.041	.025	
	1435:86	WE	25.0	1.7	1.6	.448	.019	.012	
	1435:86	WE	16.0	2.7	2.1	.626	.050	.035	
Oct. 22	1335:44	UN	14.7	.5	.5	1.257	.018	.018	
Oct. 23	1635:10	UN	39.8	9.2	6.3	0.383	.043	.028	
	1635:10	UN	17.7	3.3	2.4	1.058	.092	.072	
Oct. 24	1535:57	UN	32.0	16.5	8.0	.679	.130	.090	
	1535:57	UN	23.4	8.5	4.9	.479	.069	.047	
	1535:57	UN	21.6	1.5	1.0	.538	.024	.015	
Oct. 25	1635:02	UN	22.1	.7	.7	.413	.015	.015	x
	1635:02	UN	19.8	.6	.6	.483	.015	.015	x
	1635:02	UN	17.6	.6	.6	.513	.015	.015	x
Oct. 27	0435:57	UN	33.4	8.8	5.7	.616	.070	.051	
	0435:57	UN	16.2	3.3	2.2	1.014	.090	.070	
	0435:57	UN	8.65	.15	.15	1.279	.017	.017	x
Oct. 30	0635:89	UN	16.1	.5	.5	.989	.018	.018	x
	0635:89	UN	15.1	.5	.5	1.076	.018	.018	x
Apr. 9, 1959	1635:25	SE	7.8	.4	.4	1.308	.016	.016	x
Apr. 11	1835:44	UN	25.8	10.2	5.9	.660	.104	.073	
	1835:44	UN	16.1	2.9	2.1	.644	.051	.035	
June 25	0835:19	BY	6.5	.5	.5	1.240	.025	.025	x
27	0835:63	BY	31.4	8.6	5.3	.337	.045	.029	
	0835:63	BY	18.3	4.3	2.8	.598	.058	.042	
July 15	1235:22	ST	57.5	11.5	7.5	.226	.028	.014	
	1235:22	ST	45.7	14.8	8.2	.260	.041	.024	
July 17	1235:58	ST	54.8	13.2	8.8	.216	.020	.017	
	1235:58	ST	26.4	4.6	3.3	.384	.034	.021	
July 18	1035:22	BO	22.2	1.8	1.5	.453	.021	.015	
July 19	0835:73	BY	23.7	9.5	5.1	.372	.064	.041	
July 20	0535:47	BY	9.6	.7	.7	.832	.030	.025	
	0535:47	BY	5.00	.15	.15	.857	.015	.015	x
July 21	1335:23	BY	30.8	7.2	4.3	.334	.036	.022	
	1335:23	BY	12.8	.7	.6	.802	.022	.017	

TABLE 2. (Continued)

Date	UT	Station	f_n, kc	f_n Error +	f_n Error −	t_n, sec.	t_n Error −	t_n Error +	Actual Nose
Aug. 16, 1959	1235:20	BY	38.7	11.6	6.7	.305	.044	.028	
Aug. 17	0435:70	BY	22.6	11.3	5.1	.366	.072	.047	
	0435:70	BY	20.1	6.1	3.5	.586	.072	.053	
Aug. 17	1035:78	WE	19.4	4.7	3.2	.610	.073	.052	
Aug. 18	0935:101	BO	35.7	27.1	10.4	.179	.059	.034	
	0935:101	BO	19.0	2.3	1.7	.293	.023	.012	
	0935:101	BO	15.9	1.9	1.3	.327	.024	.013	
Aug. 18	1235:59	SE	41.8	14.2	7.8	.158	.032	.017	
	1235:59	SE	16.6	2.9	2.0	.350	.033	.019	
	1235:59	SE	15.0	.7	.7	.403	.015	.015	x
Aug. 19	1135:104	BY	31.3	6.7	4.3	.356	.037	.023	
Aug. 19	1235:27	ST	42.6	9.4	6.1	.270	.032	.018	
Aug. 19	1435:07	WE	31.2	7.3	4.7	.240	.032	.018	
Aug. 20	0635:59	SE	14.3	2.0	1.6	.824	.050	.037	
Aug. 20	0635:58	WE	13.3	1.3	1.2	.847	.040	.030	
Sept. 5	0435:44	BY	17.2	1.1	.8	.618	.020	.010	
Sept. 8	0935:37	BY	6.0	.4	.4	1.139	.015	.015	x
Nov. 23	2235:34	SE	15.2	.9	.9	1.000	.025	.025	
	2235:34	SE	12.8	.8	.8	1.207	.030	.027	
	2235:34	SE	9.9	.7	.6	.596	.020	.013	
Jan. 21, 1960	1335:61	ST	24.1	2.9	2.2	.594	.035	.024	
Apr. 1	0535:14	ST	37.9	21.1	9.1	.538	.110	.075	
Apr. 1	0735:14	BY	14.6	2.7	1.9	.589	.049	.033	
Apr. 2	0935:80	ST	17.7	8.0	3.9	.463	.081	.054	
Apr. 3	1235:29	SE	12.1	1.2	.9	.569	.028	.019	
Apr. 3	1235:21	ST	12.1	1.4	1.2	.609	.035	.024	
Apr. 4	0935:24	ST	36.6	17.0	8.1	.349	.065	.042	
Apr. 5	1235:67	ST	34.2	12.6	7.2	.386	.063	.042	
Apr. 17	0735:32	ST	34.9	4.1	3.1	.262	.021	.012	
Apr. 25	1035:23	ST	39.1	8.9	5.6	.283	.024	.020	
	1035:23	ST	18.6	2.2	1.7	.615	.035	.024	
	1035:23	ST	11.7	1.3	1.0	.921	.044	.035	
May 2	1235:56	ST	34.8	9.4	5.7	.288	.037	.022	
June 1	1235:115	ST	37.0	11.0	6.4	.354	.050	.032	
	1235:115	ST	35.2	22.0	9.5	.370	.088	.055	
June 3	1135:36	ST	28.0	14.5	7.6	.413	.083	.055	
June 29	1935:10	BY	6.25	.50	.50	.731	.115	.115	x
	1935:10	BY	4.15	.20	.20	.962	.115	.115	x
	1935:10	BY	2.45	.10	.10	1.423	.115	.115	x
July 15	1035:51	SE	8.2	.8	.8	1.400	.019	.019	x
Oct. 4	1035:55	ST	45.2	5.4	4.5	.228	.020	.010	
	1035:55	ST	40.0	4.6	3.2	.244	.020	.010	
Oct. 6	1250:100	ST	16.5	6.0	3.1	.477	.070	.047	
Oct. 7	1150:115	ST	24.0	1.5	1.5	.506	.050	.050	x
Oct. 8	1250:45	ST	22.2	4.9	3.2	.304	.035	.020	
Jan. 17, 1961	0850:12	SE	8.3	.3	.3	1.262	.016	.016	x
	0850:12	SE	6.60	.25	.25	1.523	.015	.015	x
	0850:12	SE	6.35	.20	.20	1.649	.016	.016	x
Jan. 18	0650:93	SE	8.5	.3	.3	1.523	.017	.017	x
Mar. 9	0650:39	ST	31.4	10.6	5.6	.378	.055	.036	
Mar. 12	0650:15	ST	40.7	3.3	2.8	.323	.021	.011	
	0650:15	ST	37.3	2.6	2.8	.332	.021	.012	
Mar. 30	0750:107	ST	17.5	4.3	2.9	.818	.083	.065	
Apr. 17	1050:10	SE	6.8	.2	.2	0.941	.017	.017	x
	1050:10	SE	5.55	.15	.15	1.002	.015	.015	x
	1050:10	SE	5.55	.15	.15	1.038	.015	.015	x

data near sunspot maximum, the result is a ratio in t_n of roughly 2.5:1. A horizontal line covering this 90 per cent range has been drawn near $f_n = 9$ kc/s.

The behavior of the (f_n, t_n) values from magnetically disturbed periods is impressive in its consistency. Some 31 such periods are represented by the 108 circled points, and the largest number of points from a single storm is 15 (August 16–17, 1959). The bulk of the circled points (meaning $K_p \geq 6$ at least once in the preceding 72 hours) lie on the low t_n side of the distribution. In the latitude range $\theta_0 < 58°$ ($f_n > 8$ kc), very few uncircled points are seen on the low side of the distribution, and none is seen near the greatly depressed values of t_n. It is interesting to note that, of some 7 uncircled points appearing at relatively low values of t_n, 6 lie in the region of $\theta_0 > 56°$. Although this is not emphasized in the present report, there is a general tendency toward larger and more frequent variation in t_n for the higher latitudes.

Some 15 relatively high values of t_n are circled, but of these, 10 are from periods that also exhibit 1 or more relatively low values, 4 show only a single 3-hour K_p of 6 in the preceding 72 hours, and 1 shows a maximum K_p of 7 in that period. Significantly, all 15 of the high values are from the October-April period, when typical values of t_n are grouped at the high side of the distribution.

Description of Figure 3. Whistler activity during the period June 1 to September 8, 1959 is illustrated in Figure 3. The data are taken from Figure 2, but the manner of presentation is altered slightly. Values of (f_n, t_n) from a single whistler are connected by lines. The circled values signify the use of extension methods, while squares indicate observations of actual noses. There are represented some 61 measurements from 21 recording days. Some 29 of the points represent four storm periods: the moderately severe storms ($K_p = 6$ or 7) of June 24 and September 3–6; the severe storms ($K_p =$ 8 or 9) of July 15–18 and August 16–17. These points are identified by the symbols listed in the figure.

Discussion of Figure 3. If Figure 3 is regarded as typical of the June–August period, the 90 per cent variation in t_n during that season may be estimated to be roughly in the ratio of 1.7:1. A horizontal flag exhibiting the ratio in f_n of 1.7:1 has been drawn in Figure 3 near $f_n = 12$ kc/s.

Consider the effect of magnetic storms on the data.

The August storm shows a reduction in t_n from the center of the 'typical' distribution by a factor of roughly 2. The greatly depressed values of August 18 should be compared with the flag showing the 90 per cent range for the season. While the left end of the flag is reduced from the center of the distribution by a factor of 1.3, the depressed points are lower than the left end of the flag (properly shifted) by a factor of 1.5!

The dramatic difference in appearance between the whistler records of August 18 and those from 'normal' periods is shown in Figure 1. The upper record illustrates two closely spaced multicomponent whistlers recorded at Seattle during a period of moderate activity (but no $K_p \geq 6$ in the preceding 72 hours). The record of August 18 shows a single multicomponent whistler recorded at Seattle, and illustrating the deepest part of the observed depression. The causative atmospherics on the two sets of records are aligned, and great differences in time delay at equivalent nose frequencies may be seen. The trace next to the last on the record of August 18 exhibits a nose at 15 kc/s (detected by careful examination of the records, including comparison with other events from the same recording period).

The storms of June, July, and September exhibit values of t_n that are consistently on the low side of the distribution. The July storm exhibits one highly depressed value near $f_n =$ 5 kc. Note that in this case, the same whistler shows a value of t_n near $f_n = 10$ kc that is relatively much nearer to the group of 'typical' values. This sharp departure from the component-to-component relations usually observed in whistlers has recently been investigated by the author, and many examples of this and similar effects have been found during disturbed periods. In the bulk of the cases, the traces associated with the higher latitudes show the greater depressions, as in the case illustrated.

Experimental error. Since this is only a preliminary report, an elaborate discussion of error will not be undertaken at this time. The relatively large errors assigned in Table 2 to

some of the values of (f_n, t_n) deserve comment, however.

First of all, the errors assigned to both directly observed and calculated values of (f_n, t_n) are 90 per cent errors—that is, they represent the ranges that are believed to embrace the true values with a probability of 0.9.

It should also be noted that when a value of of (f_n, t_n) is observed directly, the errors in f_n and t_n are essentially independent of one another, but that when a value of (f_n, t_n) is obtained by extension methods, the uncertainties in f_n and t_n are not independent. The latter situation is due to the nature of the measurements involved and the functional relation between f and t that underlies the calculation of (f_n, t_n) [*Smith and Carpenter*, 1961]. Thus, when a second observer making a similar set of measurements calculates a higher value of f_n than the first, the value of t_n he obtains will in most cases be lower than that found by the first observer. In Table 2, this link between the errors in f_n and t_n is expressed by associating the minus (plus) error column for t_n with the plus (minus) error column for f_n. The four values of error listed for any one case are in effect the coordinates of the end points of a single error range (for the extension method only).

Figure 4 illustrates in a simplified way the uncertainties associated with a representative set of points from Figure 3. As a convenient source of reference for variations in t_n at fixed f_n, the horizontal flag from Figure 3 showing the ratio in t_n of 1.7:1 is included.

Error flags on observations of actual noses extend vertically and horizontally. In the case of the (f_n, t_n) values derived from extension methods, a single slanting error range is shown. More detailed considerations require that these slanting flags be smeared out into a narrow region, but the effect is difficult to describe and does not qualitatively alter the picture. The larger error flags represent uncertainties in θ_0 of about 3° near $\theta_0 = 45°$ and about 1.5° near $\theta_0 = 50°$. Because the associated errors in f_n and t_n are not independent, the value of t_n for a point on a slanting error 'locus' must be considered in relation to the other t_n values at the f_n level of the point. For this reason the uncertainty in t_n tends to be small, even for the longer error flags.

A less detailed and perhaps more satisfying argument for the reliability of the extension methods is the consistency with which the data in Figure 2 above $f_n = 15$ kc/s agree with the data below that level (the latter come primarily from direct observations of nose traces).

Discussion. To what extent can the depressions in t_n be interpreted as other than first order changes in electron density? A detailed discussion of physical mechanisms in the magnetosphere is beyond the scope of this report, but some simplified remarks are appropriate.

It may be suggested that the whistler data can be interpreted primarily in terms of variations in the geomagnetic field. One of the main arguments for this interpretation would require a substantial change in the average nose frequency at a whistler station at the time of large depressions in time delay. Such a change is not observed. Another argument in favor of the magnetic field interpretation would require that the larger depressions in time delay be restricted to high latitudes. This is not in fact the case, as Figure 2 demonstrates. It is true that depressed levels are seen more frequently at the higher latitudes, but this effect is commonly manifested in drastic alterations of the usual component-to-component relations of whistlers. In such cases, the data usually show very large variations over a few degrees of latitude in the relative depression in t_n, with the higher latitude traces showing the greatest depressions. Such rapid changes with latitude should be difficult to interpret as other than first order density variations.

Another argument in favor of the density interpretation is the fact that the sequence of events during storms involving large depressions is in its broad features the same as in cases involving relatively moderate ones.

Yeh and Swenson [1961] have recently obtained integrated electron densities to 1000 km from Faraday rotation measurements on the satellite Sputnik III. The authors report depressions on the order of 2 to 4 in integrated densities during magnetically disturbed periods. These results may facilitate the interpretation of the whistler data. In the future, it should be possible to make detailed studies of the relation between the F region and the magnetosphere by comparing whistler results with data from satellite transmissions.

Conclusions. We now have the first experimental evidence on the effect of magnetic storms

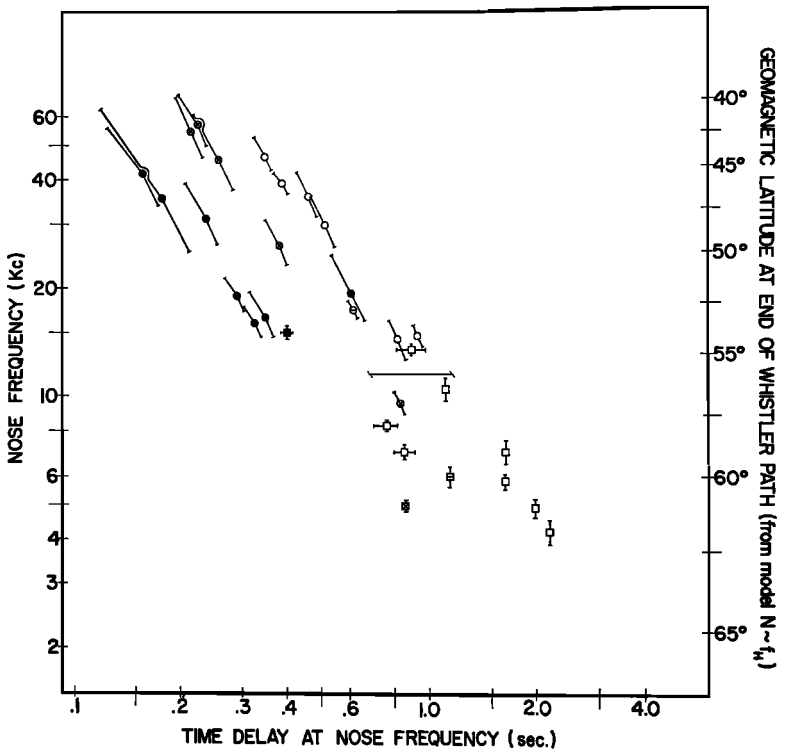

Fig. 4. The 90 per cent ranges of experimental error associated with representative values of (f_n, t_n) from Figure 3 (see discussion of error in text).

on the magnetosphere. The data show that whistler time delays at typical nose frequencies are consistently depressed during the late phases of magnetic storms, and that on some occasions the depressions in time delay are as large as 2:1 and greater. Deep depressions can be associated with nearly normal levels at near-by (usually lower) latitudes. There is strong evidence that the variations in t_n represent changes in the electron density levels in the magnetosphere. Under the density interpretation, the data show variations in electron concentration during the larger depressions that are on the order of 4:1, and a 16:1 variation over an extended period.

The prospects for further experimental work are bright, because an enormous quantity of whistler data has already been gathered, and more is continuously being obtained at a number of stations throughout the world.

Until now the only deterrent to successful use of the data has been lack of proper techniques of data analysis. Such techniques are now available and have been tested. It has become possible to use whistlers as the basis for extensive studies of the density variations in the magnetosphere.

Acknowledgments. Dr. R. A. Helliwell is to be thanked for his advice during the course of the research and his helpful comments on the manuscript. The Ellsworth data were made available through the kindness of M. G. Morgan. The assistance of Warren Nute and Ulla Lundquist in developing and applying scaling techniques, Jerry Yarbrough in making spectrograms, and John Katsufrakis in general data processing is gratefully acknowledged. Research for this paper is supported in part under Air Force contract AF18(603)-126.

References

Carpenter, D. L., Identification of whistler sources on visual records and a method of routine whistler analysis, *SEL Tech. Rept. 5,* Stanford University, March 1960.

Helliwell, R. A., and D. L. Carpenter, Whistlers-west IGY-IGC synoptic program, *SEL Final Rept.,* Stanford University, March 1961.

Helliwell, R. A., J. H. Crary, J. H. Pope, and R. L. Smith, The 'nose' whistler—a new high-latitude

phenomenon, *J. Geophys. Research, 61,* 139–142, 1956.

Smith, R. L., The use of nose whistlers in the study of the outer ionosphere, Ph.D. Dissertation, *SEL Tech. Rept. 6,* Stanford University, July 1960.

Smith, R. L., and D. L Carpenter, Extension of nose whistler analysis, *J. Geophys. Research, 66,* 2582–2586, 1961.

Storey, L. R. O., An investigation of whistling atmospherics, *Phil. Trans. Roy. Soc. A (London), 246,* 113–141, 1953.

Yeh, K. C., and G. W. Swenson, Jr., Ionospheric electron content and its variations deduced from satellite observations, *J. Geophys. Research, 66,* 1061–1067, 1961.

(Manuscript received August 17, 1961.)